

Wake potential of a charged particle in a strongly coupled two-dimensional electron gas

You-Nain Wang

*Department of Physics, University of Waterloo, Waterloo, Ontario, Canada N2L 3G1
and Department of Physics, Dalian University of Technology, Dalian 116023, People's Republic of China**

Teng-Cai Ma

Department of Physics, Dalian University of Technology, Dalian 116023, People's Republic of China

(Received 10 May 1995; revised manuscript received 31 August 1995)

The wake potential, the induced electron density, and the stopping power for a charged particle moving through a strongly coupled two-dimensional electron gas have been investigated within the framework of linear-response dielectric theory. The influence of the exchange-correlation interaction of electrons on the above quantities has been considered by using a local-field-corrected dielectric function.

I. INTRODUCTION

The interaction between charged particles and the electron gas in solids gives rise to a screened potential, with a wake dragging behind the particle. For a three-dimensional (3D) electron gas, several authors have investigated the wake potential within the framework of linear-response dielectric theory. A calculation of the wake potential was made by Neufeld and Ritchie¹ using a simple local dielectric function. A more detailed study of the wake potential within the plasmon-pole approximation was given by Ritchie, Brandt, and Echenique² and by Echenique, Ritchie, and Brandt.³ Going beyond the plasmon-pole approximation, Mazarro, Echenique, and Ritchie⁴ calculated the wake potential and the electron-gas density fluctuation in terms of the full random-phase approximation (RPA) dielectric function. In a recent paper,⁵ the wake potential in the vicinity of a solid surface has been considered.

Although much literature has been devoted to the physics of the wake potential for a 3D electron gas in past decades, to the best of our knowledge, the wake potential for a charge particle moving in an ideal two-dimensional (2D) electron gas has not been considered. In fact, a 2D electron gas can model many new materials such as copper oxide planes in high-temperature superconductors, the interface between GaAs and Ga_{1-x}Al_xAs, and the metal-oxide-semiconductor (MOS) interfaces. In recent years, some physical properties, such as the ground-state energy, correlation effects, and collective excitations for a 2D electron gas have been considered by several authors.⁶⁻⁹ In view of the importance and relevance of the 2D electron system in current experimental physics, it would be useful to investigate the interaction of the charged particles with the 2D electron system. This interaction may serve not only as a diagnostic tool for the 2D electron gas, but also as a method of changing composition of the system, such as by ion implantation.

In general, the 2D electron gas encountered in experiments in a strongly coupled system. In a recent paper,¹⁰

we have investigated the stopping power for ions moving through a 2D electron gas. It was shown that the effect of the exchange-correlation interaction in the 2D electron gas on the stopping power could be very important. It thus appears of interest to examine its effect on the wake potential.

This paper is organized in the following way. In Sec. II general formulas for the wake potential, the induced electron density, and the stopping power in a 2D electron gas are derived in the framework of linear-response dielectric theory and an expression of a local-field-corrected (LFC) dielectric function¹¹ is introduced for considering the effect of the exchange-correlation interaction. In Sec. III, numerical results of the wake potential, the induced electron density, and the stopping power are presented, and the results predicted by the LFC dielectric function are compared with those given by the RPA dielectric function. In Sec. IV, a brief summary of our results is given. In the following sections, atomic units (a.u.) with $e = m_e = \hbar = 1$ will be used.

II. GENERAL FORMULAS

We consider a point charge Z_1 moving with a constant velocity \mathbf{v} through a homogeneous 2D electron gas of density n_0 . In the present work, the quantities we are interested in are (i) the induced electric potential, the so-called wake potential, generated by the motion of the point charge, (ii) the spatial distribution of the induced electron-gas density, and (iii) the stopping power, i.e., the retarding force acting on the projectile.

Similar to the 3D case,⁴ the wake potential is given by

$$\varphi_{\text{ind}}(\mathbf{r}, t) = \frac{Z_1}{2\pi} \int \frac{d\mathbf{k}}{k} e^{i\mathbf{k} \cdot (\mathbf{r} - \mathbf{v}t)} [1/\epsilon(k, \omega) - 1], \quad (1)$$

according to the linear-response dielectric theory, where $\omega = \mathbf{k} \cdot \mathbf{v}$ and $\epsilon(k, \omega)$ is the dielectric function of the 2D electron gas. Assuming the direction of the projectile velocity \mathbf{v} to be along the x axis and employing 2D polar coordinates (k, φ) , Eq. (1) can be reduced to

$$\varphi_{\text{ind}}(\bar{x}, y) = \frac{2Z_1}{\pi v} \int_0^\infty dk \int_0^{kv} \frac{d\omega}{\kappa} \cos(\kappa y) \left[\cos \left[\frac{\omega}{v} \bar{x} \right] F_R(k, \omega) - \sin \left[\frac{\omega}{v} \bar{x} \right] F_I(k, \omega) \right], \quad (2)$$

where $\kappa = \sqrt{k^2 - \omega^2/v^2}$, $\bar{x} = x - vt$, $F_R(k, \omega) = \text{Re}[\epsilon^{-1}(k, \omega) - 1]$, and $F_I(k, \omega) = \text{Im}[\epsilon^{-1}(k, \omega) - 1]$. Here we have used the property of the dielectric function $\epsilon^*(k, \omega) = \epsilon(k, -\omega)$. One can see from Eq. (2) that the spatial distribution of the wake potential is symmetrical about the y axis.

To show the influence of the exchange-correlation interaction of the electrons in the 2D system on the wake potential, a LFC dielectric function will be used in the following discussions,

$$\epsilon(k, \omega) = 1 - P(k, \omega) / [1 + G(k)P(k, \omega)], \quad (3)$$

where $P(k, \omega)$ is the polarizability of the free-electron gas and $G(k)$ is the LFC function, which includes the effect of the exchange-correlation interaction. Using the dimensionless variables $z = k/2k_F$ and $u = \omega/kv_F$, where $k_F = (2\pi n_0)^{1/2}$ is the Fermi wave number and $v_F = k_F$ is the Fermi velocity, an analytical expression of the polarizability $P(k, \omega)$ in RPA has been given by Stern,¹²

$$P(z, u) = (\chi^2/4z^2)[f_1(z, u) + if_2(z, u)], \quad (4)$$

where

$$f_1(z, u) = -2\pi \{ 2z - C_- [(z-u)^2 - 1]^{1/2} - C_+ [(z+u)^2 - 1]^{1/2} \}, \quad (5)$$

$$f_2(z, u) = -2\pi \{ D_- [1 - (z-u)^2]^{1/2} - D_+ [1 - (z+u)^2]^{1/2} \}, \quad (6)$$

$$\begin{cases} C_\pm = (z \pm u) / |z \pm u|, \\ D_\pm = 0, \end{cases} \quad \text{for } |z \pm u| > 1, \quad (7)$$

$$\begin{cases} C_\pm = 0, \\ D_\pm = 1, \end{cases} \quad \text{for } |z \pm u| < 1, \quad (8)$$

and $\chi^2 = 1/(\pi k_F)$.

Using a sum-rule version of the self-consistent approach, Gold and Calmels¹¹ presented a parametrized expression for the LFC function $G(z)$ of the 2D electron gas,

$$G(z) = 1.982r_s^{1/3}z / [2.644C_{12}(r_s)^2 + 2r_s^{-2/3}C_{22}(r_s)^2z^2]^{1/2}, \quad (9)$$

where $r_s = (1/\pi n_0)^{1/2}$ is the electron-gas density parameter and the coefficients $C_{12}(r_s)$ and $C_{22}(r_s)$ can be found in Ref. 11.

When the projectile velocity is much less than the Fermi velocity ($v \ll v_F$), we can make the following approximations:¹⁰ $f_1(z, u) \approx -4\pi z$ and $f_2(z, u) \approx -4\pi zu / \sqrt{1-z^2}$. In this case, the wake potential along the axis of motion ($y=0$) can be simplified to

$$\varphi_{\text{ind}}(X, 0) = -2Z_1 \int_0^1 dz \{ J_0(zX) / D(z) + (v/v_F) z J'_0(zX) / [D^2(z) \sqrt{1-z^2}] \}, \quad (10)$$

where $X = 2k_F x$, $J_0(zX)$ is the zero-order Bessel function, $J'_0(x) = dJ_0(x)/dx$, and

$$D(z) = z + \pi \chi^2 [1 - G(z)]. \quad (11)$$

From Eq. (10) one sees that the first term on the right-hand side is symmetrical with respect to X , while the second term is asymmetrical.

Similarly, the corresponding induced electron density can be expressed as

$$n_{\text{ind}}(\bar{x}, y) = -\frac{Z_1}{\pi v} \int_0^\infty k dk \int_0^{kv} \frac{d\omega}{\kappa} \cos(\kappa y) \left[\cos \left[\frac{\omega}{v} \bar{x} \right] F_R(k, \omega) - \sin \left[\frac{\omega}{v} \bar{x} \right] F_I(k, \omega) \right]. \quad (12)$$

A retarding force given by $F = Z_1 \partial \phi_{\text{ind}} / \partial x$ will act on the projectile at ($x = vt, y = 0$) and cause it to lose kinetic energy. Over the length dx , the energy loss or the stopping power is given by¹⁰

$$-dE/dx = \frac{2Z_1^2}{\pi v^2} \int_0^\infty dk \int_0^{kv} \frac{\omega d\omega}{\kappa} \text{Im} \left[-\frac{1}{\epsilon(k, \omega)} \right]. \quad (13)$$

In general, contributions to Eqs. (2), (12), and (13) come from two sources: (1) the single-particle excitations in the electron gas in which $f_2(z, u) \neq 0$, and (2) the collective excitations in which $f_2(z, u) = 0$. In fact, our calculations show that the latter are much smaller than the former. In the next section, some numerical results of the wake potential, the induced electron-gas density, and the stopping power will be presented according to Eqs. (2), (12), and (13), respectively.

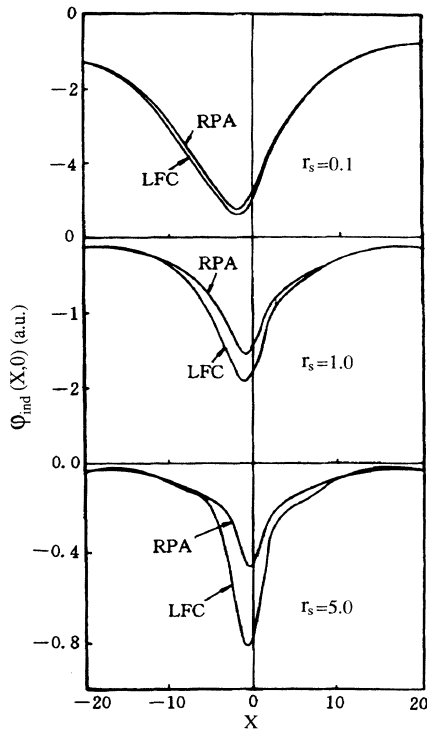


FIG. 1. The variation of the wake potential measured from a frame of reference moving with a proton ($Z_1=1$) along the axis of motion ($y=0$) for $v=0.8v_F$ and for various values of r_s . The labels "RPA" and "LFC" in the curves represent that the corresponding results are obtained by the RPA and LFC dielectric functions, respectively.

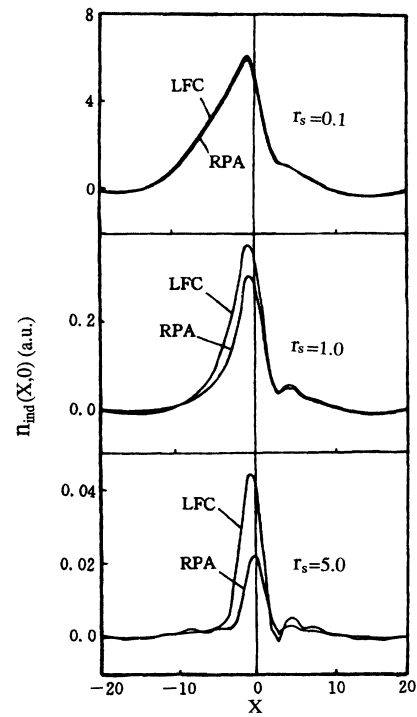


FIG. 3. The variation of the electron-gas density induced by a proton along the axis of motion for the conditions of Fig. 1.

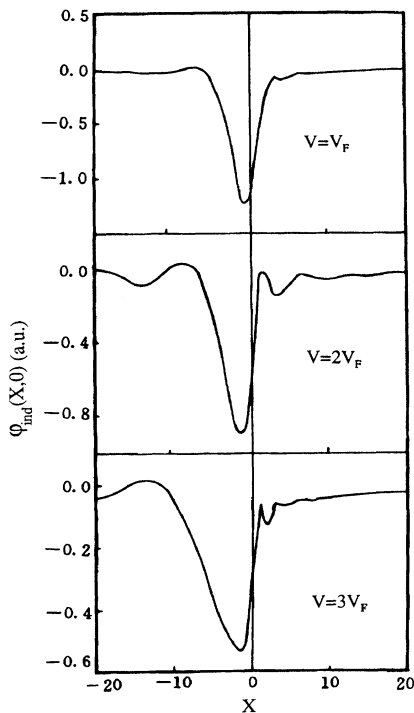


FIG. 2. The variation of the wake potential of a proton along the axis of motion for $r_s=5$ and for various values of the projectile velocity.

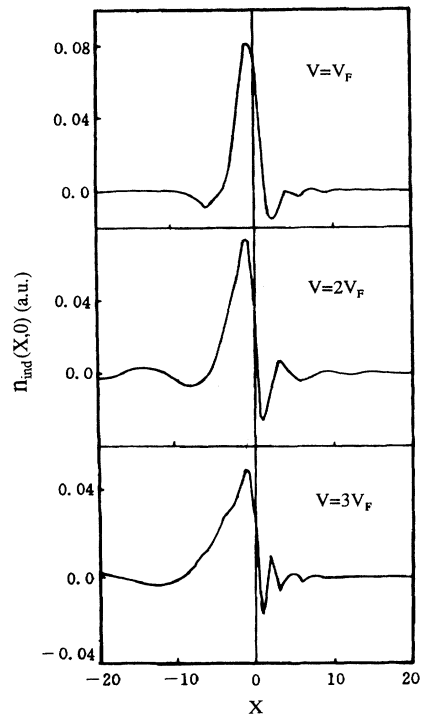


FIG. 4. The variation of the electron-gas density induced by a proton along the axis of motion for the conditions of Fig. 2.

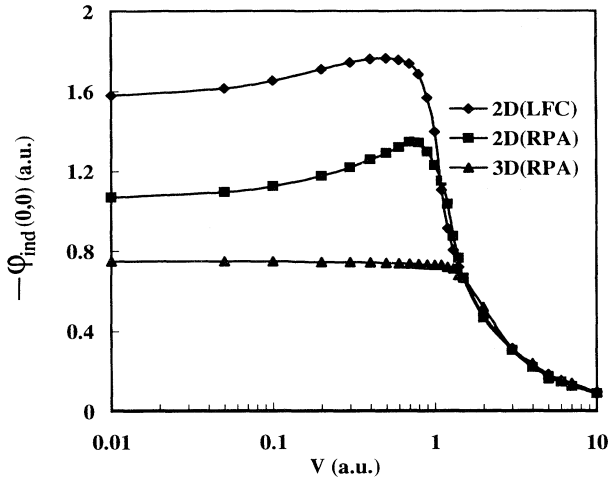


FIG. 5. The dependence of the wake potential at the origin with velocity v for $r_s=2$. The labels “2D (LFC),” “2D (RPA),” and “3D (RPA)” in the curves represent that the corresponding results are obtained by the LFC and the RPA dielectric functions of the 2D electron gas, and the RPA dielectric function of the 3D electron gas, respectively.

III. NUMERICAL RESULTS

In Fig. 1 we plot the spatial distribution of the wake potential along the axis of motion ($y=0$) measured from a frame of reference of a proton ($Z_1=1$) moving with velocity $v=0.8v_F$ in 2D electron gases with $r_s=0.1, 1.0$, and 5.0 . The labels “RPA” and “LFC” in the figure refer to the results obtained by using the RPA and LFC dielectric functions, respectively. Clearly, the exchange-correlation interaction in the electron gas enhances the values of the wake potential around $X=0$, increasing with r_s . In the low-velocity case ($v < v_F$) of Fig. 1, the asymmetry in the wake potential along the axis of motion is relatively small. In the high-velocity case ($v > v_F$) shown in Fig. 2, however, the asymmetry in the wake potential increases as the velocity increases, with oscillations in the wake potential developing in the region behind the projectile ($X < 0$).

Figures 3 and 4 show the induced electron-gas density along the axis of motion for the situations considered above. The main features observed in the wake potential are reproduced in the induced electron-gas density. In the low-velocity case, the values of the induced electron-gas density are enhanced by the exchange-correlation interaction. In the high-velocity case, the induced electron-gas density exhibits a strong asymmetry. Here, we also see that the induced electron-gas density is concentrated mainly in the neighborhood of the projectile ($X=0$). Similar to the 3D case,⁴ there are small oscillations in front of the particle, which arise mainly from the single-particle response of the medium.

In Fig. 5 we display the dependence of the wake potential at the origin with velocity for a given $r_s=2$ and compare with the 3D case. One can see that in the low-velocity case ($v < v_F$), the values of the wake potential in

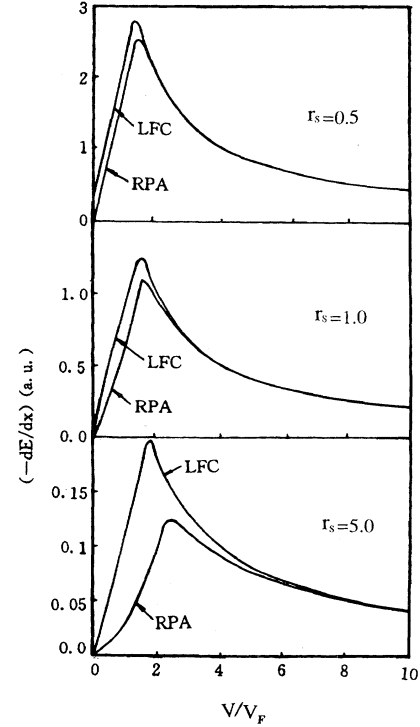


FIG. 6. The stopping power on a proton as a function of v/v_F for various values of r_s .

the 2D case are obviously larger than that in the 3D case. The asymmetry in the wake potential, and in particular, its gradient along the axis of motion at the projectile site, is the source of the stopping power. Using the RPA dielectric function, Horing, Tso, and Gumbs¹³ first evaluated the stopping power for a fast particle moving parallel to a 2D electron gas and at a height H above it. Similar calculations have also been presented by Bret and Deutsch^{14,15} for a 2D electron gas at finite temperatures. In a recent paper,¹⁰ we have presented some analytical expressions of the stopping power in both the low- and high-velocity limits. In particular, the stopping power in the high-velocity limit decreases as $1/v$, unlike the well-known form $dE/dx \propto (\ln v)/v^2$ predicted by the Bethe-Bloch formula¹⁶ in the 3D case. In Fig. 6, we display the stopping power for a proton as a function of v/v_F for $r_s=0.5, 1.0$, and 5.0 . We observe that, in the lower-velocity regime the exchange-correlation interaction has a larger effect on the values of the stopping power for larger r_s . In the high-velocity limit, however, the exchange-correlation interaction is found to have little influence on the stopping power.

IV. SUMMARY

General formulas for the wake potential, the induced electron density, and the stopping power for a charged particle moving in a 2D electron gas have been presented within linear-response dielectric theory. A LFC dielectric function is used in this work to include the effect of

the exchange-correlation interaction of the electrons within the electron gas. The numerical results show that the values of the wake potential, the induced electron-gas density, and the stopping power in the low-velocity case are enhanced by the exchange-correlation interaction, especially for the larger r_s . In the low-velocity regime, it is observed that there is a smaller asymmetry in the spatial distribution of the wake potential and the induced electron-gas density along the axis of motion. In the

high-velocity regime, however, the spatial distribution of the wake potential and the induced electron-gas density display stronger symmetries and definite oscillations.

ACKNOWLEDGMENTS

The work was supported by the Ion Beam Laboratory, Shanghai Institute of Metallurgy, Chinese Academy of Sciences. We thank R. A. Moore and W.-K. Liu for a critical reading of this manuscript.

*Permanent address.

¹J. Neufeld and R. H. Ritchie, *Phys. Rev.* **98**, 1632 (1955); **99**, 1125 (1955).

²R. H. Ritchie, W. Brandt, and P. M. Echenique, *Phys. Rev. B* **14**, 4808 (1976).

³P. M. Echenique, R. H. Ritchie, and W. Brandt, *Phys. Rev. B* **20**, 2567 (1979).

⁴A. Mazarro, P. M. Echenique, and R. H. Ritchie, *Phys. Rev. B* **27**, 4117 (1983).

⁵F. J. Garcia de Abajo and P. M. Echenique, *Phys. Rev. B* **48**, 13 399 (1993).

⁶B. Tanatar and D. M. Ceperly, *Phys. Rev. B* **39**, 5005 (1989).

⁷H. K. Sim, R. Tao, and F. Y. Wu, *Phys. Rev. B* **34**, 7123 (1986).

⁸A. Holas and K. S. Singwi, *Phys. Rev. B* **40**, 158 (1989).

⁹B. Tanatar, *Phys. Rev. B* **46**, 1347 (1992).

¹⁰Y. N. Wang and T. C. Ma, *Phys. Lett. A* **200**, 319 (1995).

¹¹A. Gold and L. Calmels, *Phys. Rev. B* **48**, 11 622 (1993).

¹²F. Stern, *Phys. Rev. Lett.* **18**, 546 (1967).

¹³N. J. M. Horing, H. C. Tso, and G. Gumbs, *Phys. Rev. B* **36**, 1588 (1987).

¹⁴A. Bret and C. Deutsch, *Phys. Rev. E* **48**, 2994 (1993).

¹⁵A. Bret and C. Deutsch, *Europhys. Lett.* **25**, 291 (1994).

¹⁶H. A. Bethe, *Ann. Phys. (Leipzig)* **5**, 325 (1930).